

Reduced graphite oxide in supercapacitor electrodes

Belén Lobato ^a, Viliam Vretenár ^{b,c}, Peter Kotrusz ^b, Martin Hulman ^{b,d}, Teresa A. Centeno ^{a*}

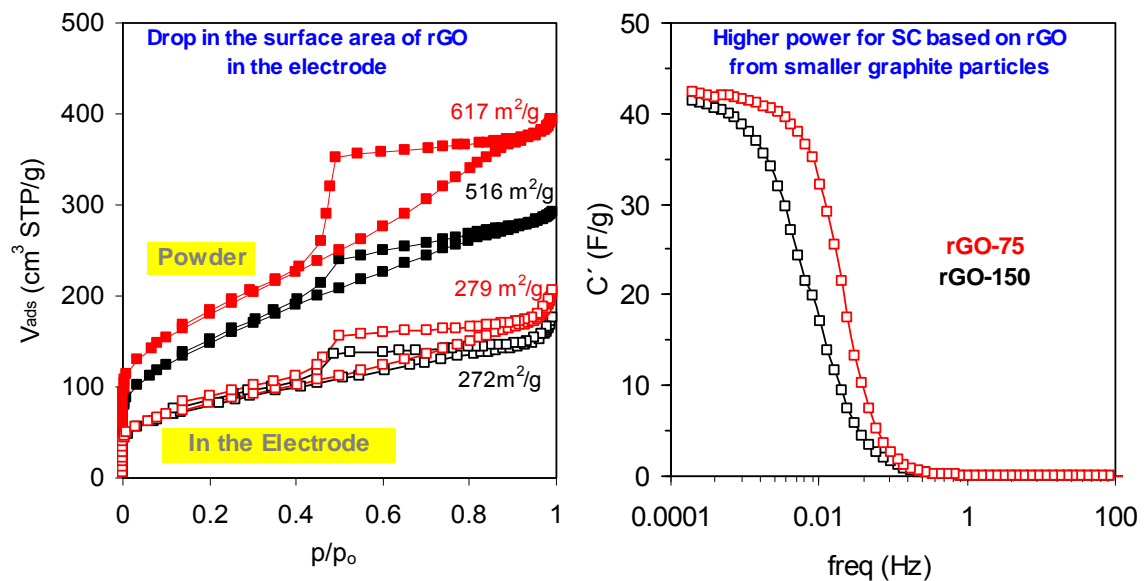
^a Instituto Nacional del Carbón-CSIC, Apartado 73, 33080 Oviedo, Spain

^b Danubia NanoTech, s.r.o., Ilkovicova 3, 841 04 Bratislava, Slovakia

^c STU Centre for Nanodiagnosics, Vazovova 5,812 43 Bratislava, Slovakia

^d Institute of Electrical Engineering, SAS, Dúbravská cesta 9, 841 04 Bratislava, Slovakia

Graphical abstract



* Corresponding author. Tel.: +34 985119090; Fax: +34 985297662.

E-mail address: teresa@incar.csic.es (T.A. Centeno)

Abstract

The current energy needs have put the focus on highly efficient energy storage systems such as supercapacitors. At present, much attention focuses on graphene-like materials as promising supercapacitor electrodes.

Here we show that reduced graphite oxide offers a very interesting potential. Materials obtained by oxidation of natural graphite and subsequent sonication and reduction by hydrazine achieve specific capacitances as high as 170 F/g in H_2SO_4 and 84 F/g in $(\text{C}_2\text{H}_5)_4\text{NBF}_4/\text{acetonitrile}$. Although the particle size of the raw graphite has no significant effect on the physico-chemical characteristics of the reduced materials, that exfoliated from smaller particles ($<75 \mu\text{m}$) result more advantageous for the release of the stored electrical energy. This effect is particularly evident in the aqueous electrolyte.

Graphene-like materials may suffer from a drop in their specific surface area upon fabrication of electrodes with features of the existing commercial devices. This should be taken into account for a reliable interpretation of their performance in supercapacitors.

Keywords: supercapacitor, reduced graphite oxide, graphene material, electrode surface

1. Introduction

Among the wide variety of carbon materials that are being studied for supercapacitor electrodes, graphene has recently emerged as the best candidate due to its outstanding specific surface area and electrical conductivity [1, 2]. Undoubtedly, it has great potential but its actual application still has many challenges. One of the most important is the industrial production of homogeneous graphene in a reproducible manner. It has been illustrated that the structural, chemical, textural and electrical properties are highly dependant on the synthesis method. Thus, the graphene materials obtained at large scale present much lower electrical conductivity and specific surface area than graphene monolayer [3-5]. Moreover, the preparation procedures have dramatic influence upon the specific capacitance [6]. From the economical point of view, graphene materials offer good performance but at high cost [7] and the supercapacitor market is much more sensitive to price than to an extraordinary behaviour [8]. In this context, activated carbons still remain much more competitive for commercial SC [7, 8].

At the present, much basic research is focused on the study of the influence of the synthesis parameters on the final characteristics of the graphene materials. The ultimate goal is to determine the key factors that lead to materials with optimal performance by easily scalable and inexpensive methods [3-5].

Graphite oxide (GO) is attracting great attention because it offers a promising route to large quantities of graphene [4,5]. The graphite intercalation with oxygen-containing groups [4,9] increases the interlayer spacing and the oxidized graphite easily exfoliates into individual graphene oxide flakes. The oxygen-functionalities cause strong electron localization shutting down the charge transport in graphene oxide [10] but its reduction by chemical or thermal processes leads to a structure close to graphene with high electrical conductivity [4].

The structural integrity of graphene may not be a priority for supercapacitor electrodes and reduced graphite oxides (rGO) obtained by oxidation of natural graphite and subsequent sonication and reduction by hydrazine offer a very interesting potential.

It is shown that the particle size of the raw graphite has a limited effect on the structural, textural and chemical features of the reduced graphite oxides. As a

consequence, rGOs from particles below 75 and 150 μm display very similar specific capacitances around 170 F/g in H_2SO_4 and 84 F/g in $(\text{C}_2\text{H}_5)_4\text{NBF}_4/\text{acetonitrile}$ at low current density.

On the contrary, the particle size of the graphite has an impact on the behavior at high frequency and particles smaller than 75 μm result more efficient for high power.

This work also illustrates a loss of 50% in the specific surface area of rGO when processed in electrodes with features of commercial devices. As comparison, an activated carbon used in commercial supercapacitors reduces its surface by only 6% in the electrode. This should be taken into account to evaluate how far the correlations between the textural properties and the SC performance found for carbons [11-13] can be applied to graphene-like materials.

2. Experimental

2.1. Materials preparation

Samples of natural graphite (Alfa Aesar) with particle sizes below 75 and 150 μm (Alfa Aesar) were subjected to chemical oxidation by the modified Hummer's method by Jeong [14]. Sulphuric acid (350 ml) was mixed with the graphite powder (2 g) at 0-5°C for 15 minutes. Potassium permanganate (8 g) and sodium nitrate (1 g) were added portion-wise at 0°C and stirred for 30 minutes and then at 35°C (30 min). Water (250 ml) was added via dropping funnel and the mixture was heated to 98°C for 3 hours. The reaction was terminated by adding 500 ml of deionized water and 40 ml of 30% H_2O_2 . The dispersion was filtered off through nylon filter, washed with diluted HCl (10 wt.%) to remove metal ions and then with water until pH of filtrate is about 7.

The oxidized samples, GO-75 and GO-150, were further sonicated and treated with hydrazine to get the reduced graphene-like materials rGO-75 and rGO-150, respectively. Deionized water (150 ml) was added to GO (1 g) and vigorously stirred for 24 hours at room temperature. The suspension was subsequently sonicated in a bath sonicator (Kraintek, 70 W, 38 kHz) for 3 hours, in a tip-probe sonicator (Hielscher UP200S, 200 W, 24 kHz) for 30 minutes and, finally, for 1 hour in the bath sonicator. The mixture was treated with ammonia (1.5 ml) and hydrazine monohydrate (3 ml) and stirred vigorously at 85°C for 24 hours under reflux condenser. After cooling, the suspension was filtered off through nylon

filter, washed with deionized water (500 ml) and with methanol (50 ml). The cake was dried at 75°C for 24 hours.

Buglione et al. [6] and Park et al. [15] have schematically illustrated the chemical transformations that occur in similar processes.

2.2 Materials characterization

The chemical characterization of the samples involved the determination of the total oxygen content and the surface functionalities by XPS whereas the structural features were studied by XRD. The textural properties were estimated from the analysis of N₂ isotherms at 77K by different methods [13]. The electrical conductivity was measured by the four-probe method using rGO compact films.

The rGO particles were processed into electrodes by rolling a mixture with 5 %wt PTFE and 5 %wt carbon black into 250 µm thick films. Discs of 8 mm in diameter and carbon loading ~ 15 mg/cm² were punched out. The electrochemical performance was tested in a two-electrode cell with a glassy fibrous paper as separator. Cyclic voltammetry tests at various scan rates (1-50 mV/s) as well as charge-discharge cycles at different current densities (1-70 mA/cm²) were performed in 2M aqueous H₂SO₄ (0-0.8 V) and 1M (C₂H₅)₄NBF₄ in acetonitrile (TEABF₄/AN, 0-2 V). Electrochemical impedance spectroscopy (EIS) measurements were performed by applying a sinusoidal signal of ± 15 mV from 2 10⁻⁴ Hz to 60 kHz.

Experimental details regarding preparation and characterization of the samples are summarized in the Supporting Information (SI).

3. Results and discussion

It appears that the particle size of the raw graphite has no significant influence on the chemical composition of the materials obtained through Hummer-Jeong oxidation. Both GO-75 and GO-150 display total oxygen content of around 51% and similar surface groups (Figs. 1a and S1). The major difference is a somewhat higher presence of C-O functionalities in the material derived from smaller particles.

On the contrary, the structural expansion induced by the oxygen-functionalities and water intercalated between the graphitic layers is notably affected by the

size of the raw particles (Fig. 1b). The XRD spectrum of GO-75 displays an intense peak (001) at 10.7° indicating the increase in the interlayer spacing by a factor of 2.5 (0.83 nm) compared to that of the starting graphite (0.335 nm). The less intense and broader signal at 20.7° suggests that the intercalation is not homogeneous since GO-75 also contains disordered regions with a wide range of spacing (centered at ~ 0.43 nm).

The expansion by oxidation is more limited when larger graphite particles are used; the XRD peak observed for GO-150 at 12.4° corresponds to a smaller interlayer distance (0.72 nm) than that in the GO-75 sample whereas the very broad signal around 23° reveals some amount of a highly disordered carbon structure.

The treatment with hydrazine reduces both oxidized samples quite efficiently and the structural differences observed for GOs are not significantly reflected in the reduced materials. The oxygen content drops to 17-18 % for rGO-75 and rGO-150 although XPS analysis suggests that the reduction is somewhat more effective for the latter. Its spectrum displays only one asymmetric peak due to sp^2 hybridized carbon whereas that for rGO-75 still shows a weak signal associated to oxygen groups (Figs. 1a and S1).

The successful reduction is confirmed by the disappearance of the (001) peak in the XRD patterns of rGOs (Fig. 1b). The partial reappearance of signals at around 24.4° and 43° indicates, respectively, that agglomeration and re-staking of graphene oxide items occur to some extent during filtering/drying processes, being favored by smaller particles.

The entanglement and overlap of the rGO flakes lead to a notable porosity and specific surface areas as high as $617 \text{ m}^2 \text{ g}^{-1}$ for rGO-75 and $516 \text{ m}^2 \text{ g}^{-1}$ for rGO-150 are achieved. The shape of the N_2 isotherms (Fig. 2a) is typical type IV and reflects the mesoporous character of both rGOs. The well-defined capillary condensation step at $p/p_0 \sim 0.4-0.8$ observed for rGO-75 reveals an interconnected network of mesopores of different shape and size below 20 nm. In the case of the material with larger particles rGO-150, the hysteresis loop is given by slit-type pores smaller than 10 nm. The analysis by the Dubinin-Radushkevich equation reports that 40 % of the total pore volume of rGOs corresponds to wide micropores with an average size of 1.5-1.6 nm.

Despite the large concentration of structural defects [16] introduced by the hydrazine treatment, the electrical conductivity of our chemically reduced samples is recovered sufficiently up to around 1 S/cm. Figs. 3 and 4 illustrate that reduced graphite oxide is a material indeed adequate for the energy storage in SC. The charge-discharge curves at different current densities show good symmetry and linear slopes, which is indicative of efficient electrochemical double layer formation in both aqueous H_2SO_4 (Fig. 3a) and TEABF_4 in acetonitrile (Fig. 4a) electrolytes. The rectangular shape of the cyclic voltammograms (Fig. 3b and 4b) confirms a near-ideal capacitive behaviour with good rate performance.

The potential of the reduced graphite oxides in SC is suggested by their specific capacitance at 1 mA/cm^2 , around 170 F/g in the H_2SO_4 and 84 F/g in the organic medium (Table 1), which is comparable with those of highly porous activated carbons [11-13] and materials obtained by standard chemical reductions of graphene oxide [3, 4].

It is worth noting that both samples reach similar limiting capacitance although their specific surface is quite different. N_2 adsorption isotherms performed on the rGO-electrodes (Fig. 2a) reveal the existence of further agglomeration and re-stacking of the powdered materials upon electrode processing and their surface area drops to only 270 m^2/g , regardless of the particle size. Therefore, the specific surface area determined for the graphene materials in powder may be misleading as it does not correspond to the effective surface available in the electrode. Moreover, this should be also considered for the interpretation of the performance of graphene materials within the general patterns reported for standard carbons [11-13]. As illustrated by Fig. 2b, the biomass-based activated carbon Picatif SC, developed by PICA (France) for supercapacitor electrodes, decreases its surface area by only 6% in the electrode. As previously reported [13], in the case of Picatif SC which displays large micropores above 1 nm, the BET equation overrates the real surface area. Its specific surface was obtained from the average of the values obtained by Dubinin's theory, DFT approach and comparison plot.

While the particle size does not affect the SC behavior at low intensities, it has an impact on the high power performance. Table 1 shows that the change of current density from 1 to 70 mA/cm^2 reduces the specific capacitance of rGO-75

in 29% in H_2SO_4 and 20% in TEABF_4/AN . For rGO-150, the capacitance decrease is 75% and 51%, respectively.

The better capacitance retention observed for the reduced graphite oxide from smaller particles correlates with its faster performance observed by EIS. Figs. 3c and 4c illustrate that the device based on rGO-75 displays a nearly ideal capacitive behavior with a marked vertical slope at the low-frequency region. By contrast, larger particles lead to a higher electrode resistance as well as to the enhancement of diffusional restrictions for ions adsorption.

Interestingly, the influence of the particle size on the ability to operate at high frequency is more evident in the aqueous electrolyte despite having smaller ions. As shown by Fig. 3d, the material with smaller particles achieves capacitance saturation at higher frequency and its response is much faster. The maximum operating frequency f_{max} (at which the capacitance drops to 50% of its maximum value) of rGO-75 is 2.9 higher than that of rGO-150. With H_2SO_4 as electrolyte, the ions mobility is also hindered by slow redox reactions involving oxygen functionalities on the carbon surface [17] and its effect is more marked in larger particles.

In TEABF_4/AN , the interactions with the surface groups are less relevant and rGO-75 demonstrates somewhat better frequency response than rGO-150 due to shorter paths lengths in smaller particles.

4. Conclusions

Reduced graphite oxide is an interesting candidate for SC electrodes, achieving specific capacitances as high as 170 F/g in aqueous H_2SO_4 and 84 F/g in $(\text{C}_2\text{H}_5)_4\text{NBF}_4/\text{acetonitrile}$.

The specific surface area determined for graphene-like materials in powder may be misleading as it does not reflect the available surface in the electrode. The problem arises during the fabrication of electrodes matching the thickness and the carbon loading of commercial devices where rGOs experience a drop in their surface area of around 50%. On the other hand, this reduction is only 6% in the case of the activated carbon Picatif SC used in commercial devices. This should be addressed for a coherent interpretation of the performance of graphene materials within the general behavior reported for carbon-based SC.

The size of the raw graphite has no relevant effect on the physico-chemical characteristics of the reduced graphite oxides. As a consequence, rGOs from particles below 75 and 150 μm in size display very similar supercapacitor performance at low current density. On the contrary, the material exfoliated from smaller particles results more advantageous for the release of the stored electric energy. This effect is particularly noticeable in the aqueous electrolyte.

Acknowledgements

Financial support from EU 7FP [Project Electrograph-266391], the project VEGA 1254/12 (M.H.) and MICINN [MAT 2011-25198] (T.A.C.) is gratefully acknowledged. The authors are grateful to Prof. Viera Skákalová for the useful discussions and critical remarks.

References

- [1] Y. Zhai, Y. Dou, D. Zhao, P.F. Fulvio, R. T. Mayes, S. Dai, *Adv. Mater.* 23 (2011) 4828-4850.
- [2] Y.B. Tan, J-M. Lee, *J. Mater Chem. A* 1 (2013) 14814-14843.
- [3] Y. Huang, J. Liang, Y. Chen, *Small* 8 (2012) 1805-1834.
- [4] Y. Zhu, S. Murali, W. Cai, X. Li, J.W. Suk, J. R. Potts, R.S. Ruoff, *Adv. Mater* 22 (2010) 3906-3924.
- [5] C. Soldano, A. Mahmood, E. Dujardin, *Carbon* 48 (2010) 2127-2150.
- [6] L. Buglione, E.L.K. Chng, A. Ambrosi, Z. Sofer, M. Pumera, *Electrochem. Commun.* 14 (2012) 5-8.
- [7] E. P.Randviir, D.A.C. Brownson, C.E. Banks, *Mater. Today* 17 (2014) 426-432.
- [8] L. Weinstein, R. Dash, *Mater. Today* 16 (2013) 356-357.
- [9] H.-P. Boehm, *Angew. Chem. Int. Ed.* 49 (2010) 9332-9335.
- [10] V. Skákalová, V. Vretenár, Ľ. Kopera, P. Kotrusz, C. Mangler, M. Meško, J. C. Meyer, M. Hulman, *Carbon* 72 (2014) 224-232.
- [11] T. A. Centeno, F. Stoeckli, *Electrochim. Acta* 52 (2006) 560-566.
- [12] T. A. Centeno, M. Hahn, J. A. Fernández, R. Kötz, F. Stoeckli, *Electrochem. Commun.* 9 (2007) 1242-1246.
- [13] F. Stoeckli, T.A. Centeno, *J. Mater. Chem. A* 1 (2013) 6865-6873.
- [14] T. A. Pham, J. S. Kim, J. S. Kim, Y. T. Jeong, *Colloids and Surfaces A: Physicochem. Eng. Aspects*, 384 (2011) 543-548.
- [15] S. Park, J. An, J.R. Potts, A. Velamakanni, S. Murali, R.S. Ruoff, *Carbon* 49 (2011) 3019-3023
- [16] C. Gomez-Navarro, J. C. Meyer, R. S. Sundaram, A. Chuvilin, S. Kurasch, M. Burghard, K. Kern, U. Kaiser, *Nano Letters* 10 (2010) 1144-1148.
- [17] B.E. Conway, *Electrochemical Supercapacitors*, Vol. 1, Kluwer Academic/Plenum Publishers, New York 1999.

Table 1. Specific capacitance (F/g) of the reduced graphite oxides at different current densities (mA/cm²). The values are relative to the rGO mass in a single electrode.

Reduced graphite oxide	H ₂ SO ₄				TEABF ₄ /AN			
	1	10	30	70	1	10	30	70
rGO-75	170	155	143	121	86	81	75	69
rGO-150	168	143	96	41	82	74	62	40

Fig. 1. XPS (a) and XRD (b) spectra for the graphite oxides (GO) and the reduced graphite oxides (rGO).

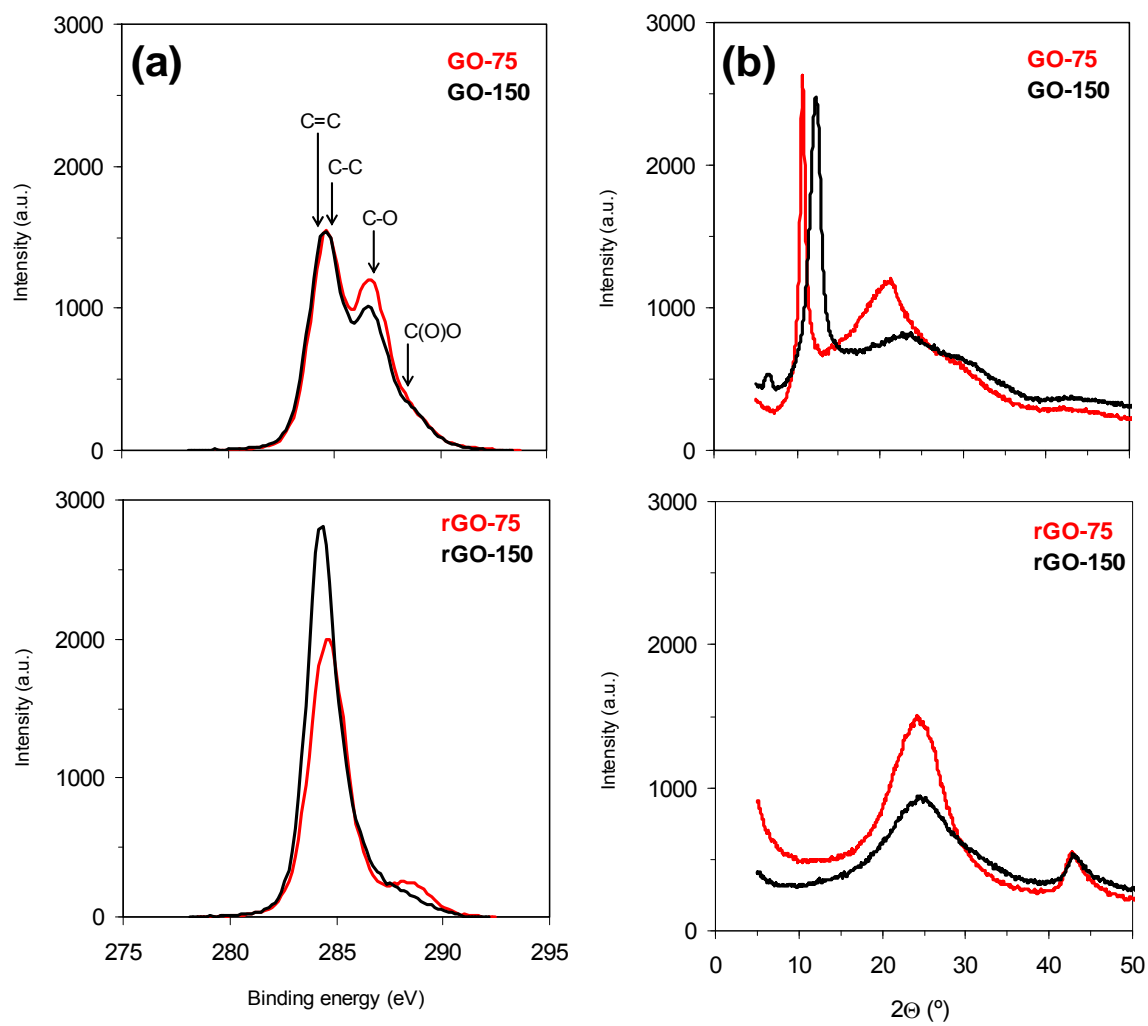


Fig. 2. N₂ isotherm of rGOs and the activated carbon Picactif SC in powder and in the electrode (the adsorbed volume is referred to carbon mass in the samples). As BET equation overrates the real surface area of Picactif [13], the values for this material correspond to the average of the other more reliable determinations.

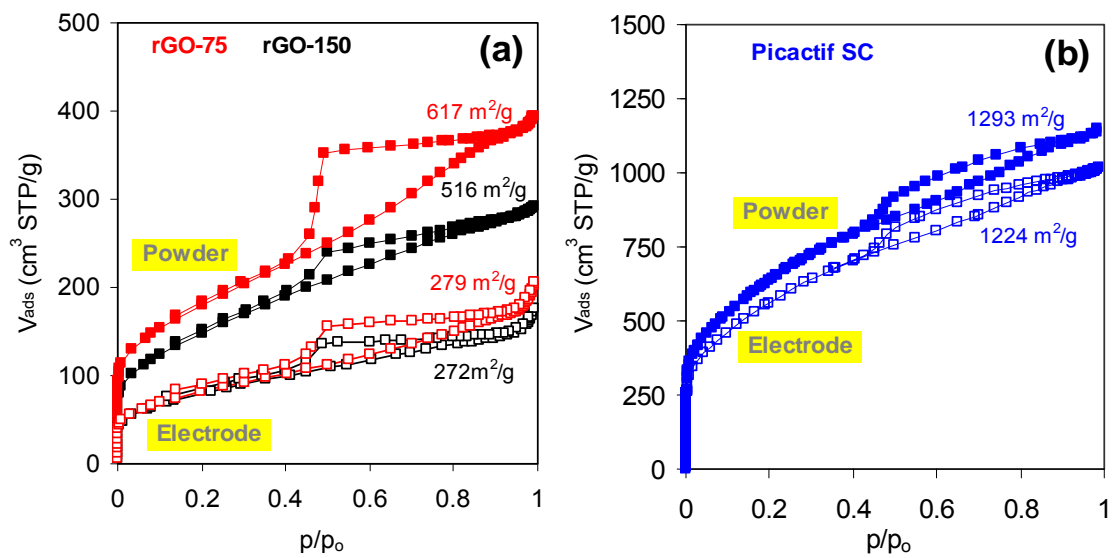


Fig. 3. Electrochemical performance of the reduced graphite oxides in 2M H_2SO_4 . a) Galvanostatic charge-discharge cycles at 5 mA/cm^2 , b) Cyclic voltammograms at 1 and 10 mV/s , c) EIS Nyquist plot (high-frequency range), d) Evolution of the normalized capacitance C/C_{max} with the frequency.

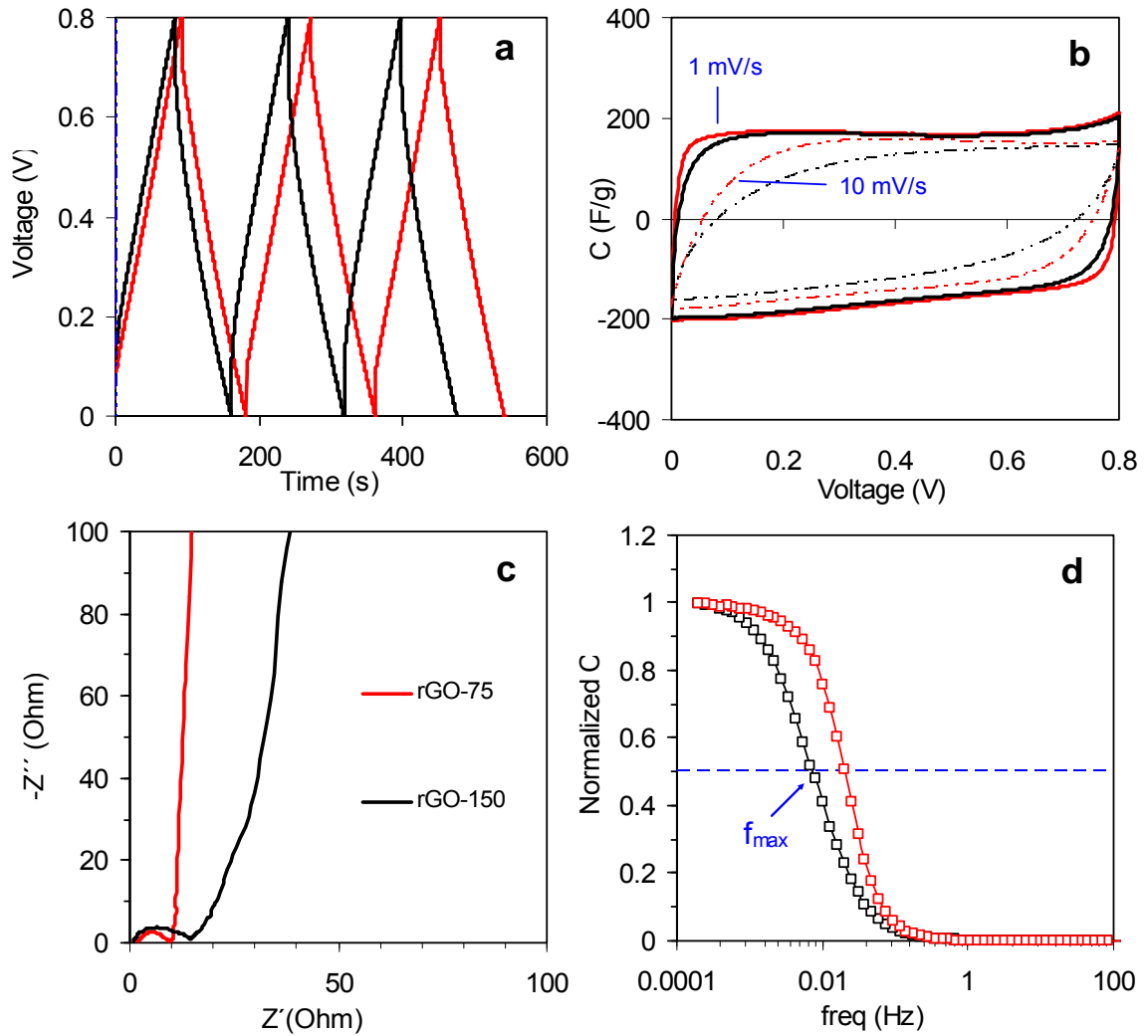
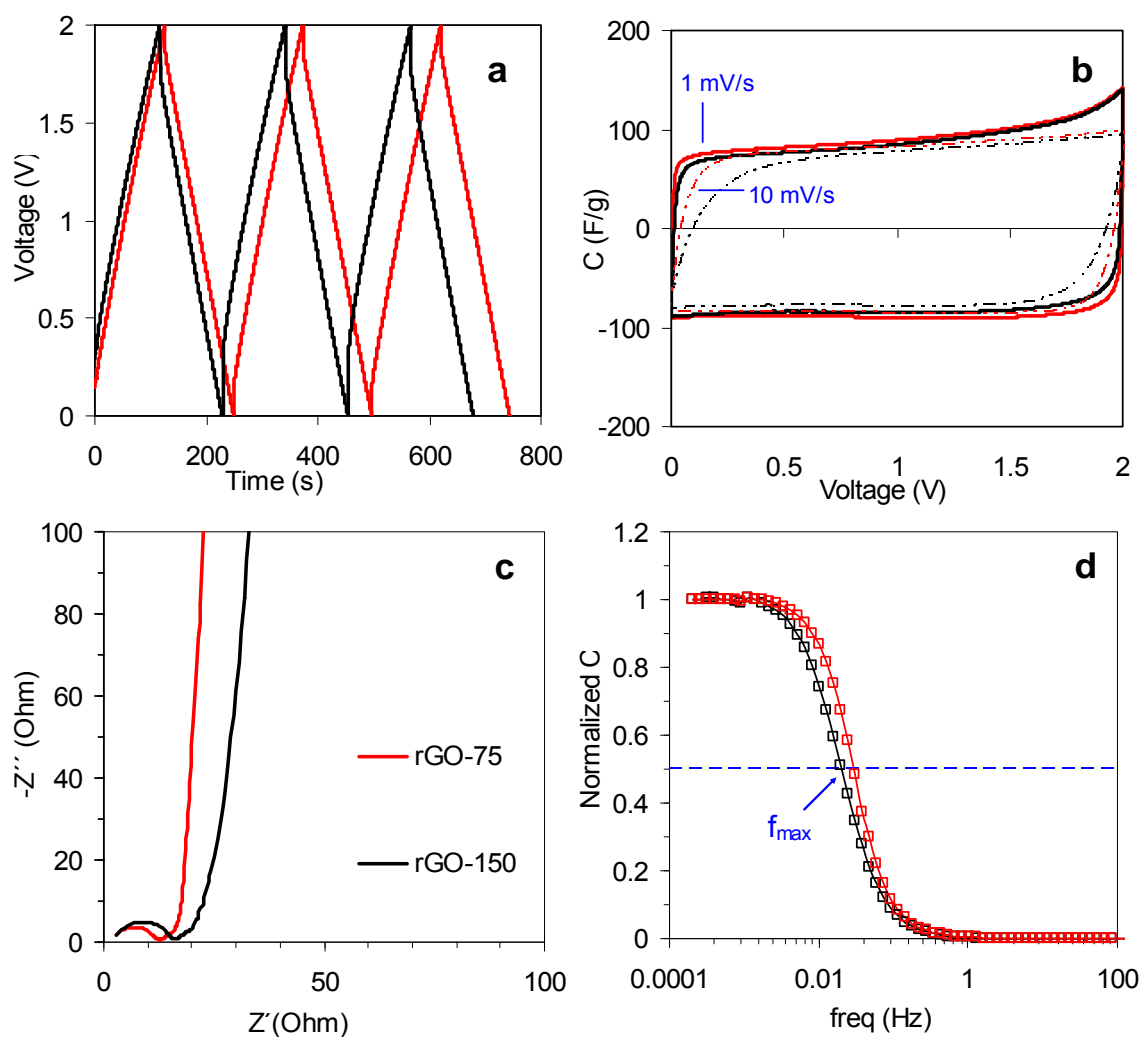


Fig. 4. Electrochemical performance of the reduced graphite oxides in 1M TEABF₄/AN. a) Galvanostatic charge-discharge cycles at 5 mA/cm², b) Cyclic voltammograms at 1 and 10 mV/s, c) EIS Nyquist plot (high-frequency range), d) Evolution of the normalized capacitance C/C_{max} with the frequency.



Supporting information

Characterization of the materials

The O content in the samples was determined by a LECO-TF-900 furnace coupled to a LECO-CHNS-932 microanalyzer. The surface functionalities of the GO samples were detected by X-ray photoelectron spectroscopy (XPS) using fully automated Thermo Scientific K-Alpha XPS system. The spectra have been decomposed into four peaks centered at 284.3, 284.9, 286.7 and 288.5 eV, corresponding to carbon sp^2 , carbon sp^3 , C-O-C and COOH functional groups, respectively [1].

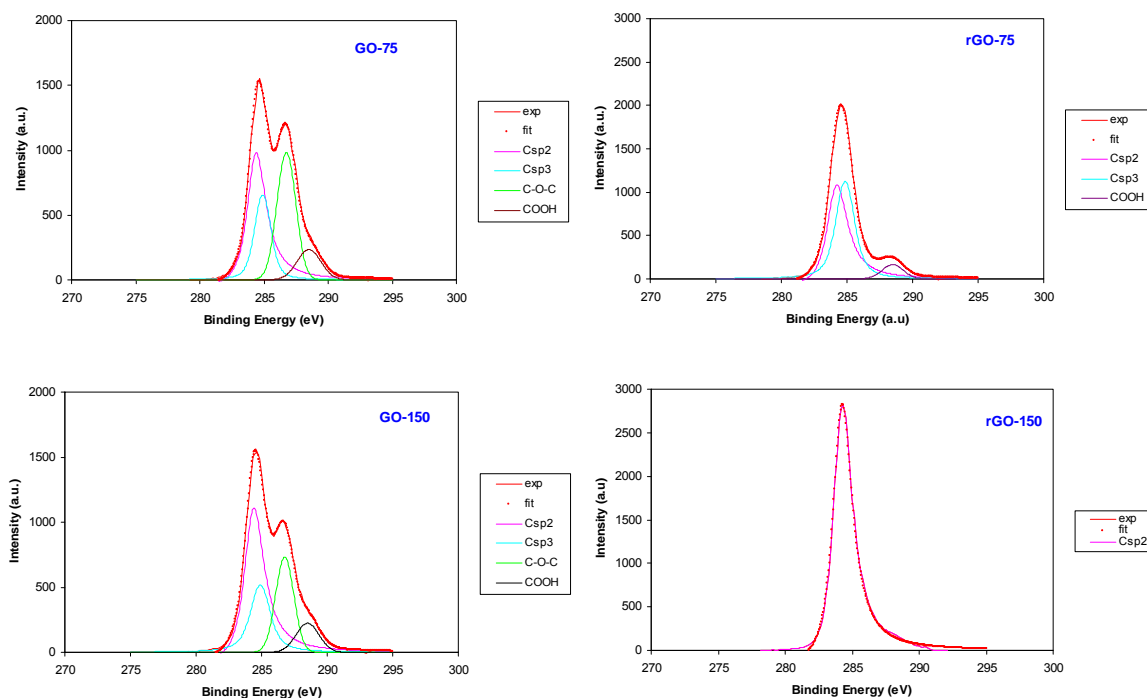


Figure S1. Deconvolution of the XPS spectrum of the materials

X-Ray Diffraction (XRD) analysis was performed by using a D5000-Siemens diffractometer ($K\alpha_1$ line from Cu (1.5406 \AA), power supply of 40 kV and 40 mA). The textural features were estimated from the analysis of N_2 isotherms at 77K (Micromeritics ASAP 2010) by different methods such as BET equation, Dubinin's theory, DFT approach and comparison plot [2]. The pore size

distributions (PSD) were obtained by applying the Kruk-Jaroniec-Sayari (KJS) method to the adsorption branch of the N₂ isotherm [3].

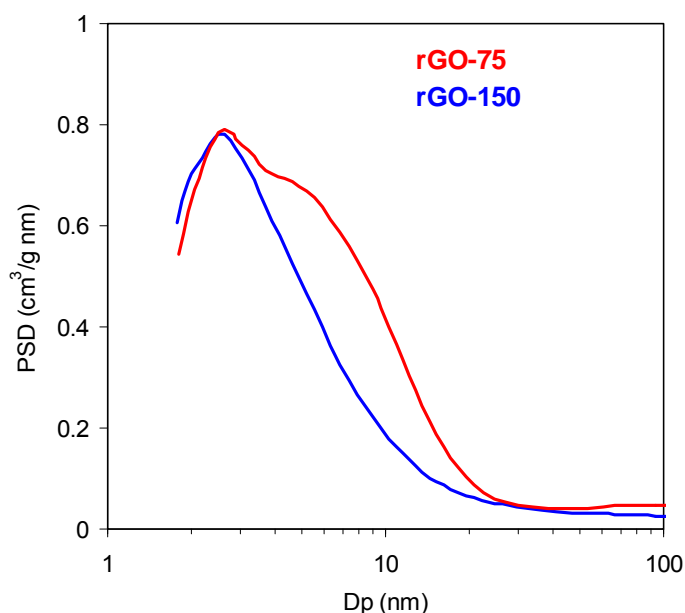


Figure S2. Pore size distribution of the reduced graphite oxides

The electrical conductivity of rGO materials was measured by the four-probe method using precise Keithley 2400 source meter. The samples were prepared in the form of compact films by vacuum filtration (measurement of in-plane conductivity) with average thickness of about 30 μm .

The rGO particles were processed into electrodes by mixing with 5 %wt PTFE and 5 %wt carbon black (Super P). The mixture was homogenized in an agate mortar, formed into electrodes by rolling it into 250 μm thick film, and finally by punching out 8 mm diameter discs. The carbon loading was $\sim 15 \text{ mg/cm}^2$. The electrochemical performance was tested in a two-electrode cell with rGO pellets separated by glassy fibrous paper (Whatman 934-AH).

Cyclic voltammetry (CV) tests at various scan rates (1-50 mV/s) as well as charge-discharge cycles at different current densities (1-50 mA/cm²) were performed between 0 and 0.8 V in 2M aqueous H₂SO₄ and from 0 to 2 V in the organic electrolyte 1 M (C₂H₅)₄NBF₄ in acetonitrile (TEABF₄/AN). Electrochemical impedance spectroscopy (EIS) measurements were performed by applying a sinusoidal signal of $\pm 15 \text{ mV}$ from $2 \cdot 10^{-4} \text{ Hz}$ to 60 kHz in a

PGSTAT 30 (Autolab B.V., Metrohm) potentiostat equipped with a FRA32M module.

References

- [1] Y. Yamada , H. Yasuda, K. Murota, M. Nakamura, T. Sodesawa, S.Sato, J. Mater. Sci. 48 (2013) 8171.
- [2] F. Stoeckli, T.A. Centeno, J. Mater. Chem. A 1 (2013) 6865.
- [3] M. Kruk, M. Jaroniec, A. Sayari, Langmuir 13 (1997) 6267.